Available online at www.sciencedirect.com
ScienceDirect
Journal of Crystal Growth 307 (2007) 171–176
JOURNAL OF CRYSTAL GROWTH
www.elsevier.com/locate/jcrysgro

Formation of regular zigzag branch of CsCl crystallites on glass substrate: A new lateral growth mechanism leading to long-range ordering

Wei Pan, Y.W. Mao, D.J. Shu, G.B. Ma, Mu Wang*, R.W. Peng, X.P. Hao, N.-B. Ming

National Laboratory of Solid State Microstructures and Department of Physics, Nanjing University, Nanjing 210093, China

Received 20 November 2006; received in revised form 5 April 2007; accepted 17 May 2007
Communicated by Y. Furukawa
Available online 3 June 2007

Abstract

We report in this article a mechanism to form regularly zigzag branch of CsCl crystallites on a flat glass substrate, in which the crystallographic orientation rotates continuously, and a pattern with long-range order on tens of micrometer scale is generated. Atomic force microscopy (AFM) indicates that this unusual crystallization behavior is associated with successive nucleation at the concave edge of crystallite facet and glass substrate, where interfacial tension underneath the nucleus is asymmetric. We suggest that these observations reveal a new lateral growth mode, and may help to understand a class of long-range ordering effect in crystallization.

PACS: 81.10.Aj; 81.15.−z; 64.60.Qb; 68.03.Cd; 68.37.Ps

Keywords: A1. Atomic force microscopy; A1. Nucleation; A1. Physics of crystal growth; A1. Surface tension; A3. Film growth and epitaxy

1. Introduction

Alignment of inorganic crystal on a substrate of different material has attracted much attention recently because of the motivation to search for new functional materials [1–12]. To achieve architectural control over formation of structural and functional components, templates are usually used. For example, calcium phosphate or calcium carbonate crystallites can be orderly assembled by organic matrix (substrate) to form tough, durable and adaptive polymer–ceramic composite [13,14]. Meanwhile structure of the substrate affects crystallization across the interface in selecting nucleation sites, and in controlling growth mode and crystal morphology [15–18]. However, regular structures may also be self-organized without any template. We recently observed in crystallization of NH_4Cl from agarose gel where crystallite aggregate may possess strict geometrical regularity when crystallite of NH_4Cl develops laterally on glass substrate [19–21]. It is interesting to find out how the crystallographic orientation of a crystallite is sensed by neighboring ones and how the overall morphology of the aggregate is modulated by their interactions. In addition, it is also interesting to find out how universal this phenomenon could be: whether similar growth behavior can be observed in crystallization of salts apart from NH_4Cl [19–21] and $FeSO_4$ [22].

In this article we present structural and morphological investigations on a long-range-ordering effect observed in CsCl crystallite aggregation, which originates from self-organized consecutive rotation of crystallographic orientation in lateral growth. We suggest that this effect occurs as long as lateral growth is controlled by successive nucleation on the concave edge of crystal facet and substrate. This crystallization behavior should be enlightening in understanding self-organization of ordered structures.

*Corresponding author. Tel.: +86 25 83594496; fax: +86 25 8359 5535.
E-mail address: muwang@nju.edu.cn (M. Wang).

0022-0248/$ - see front matter © 2007 Elsevier B.V. All rights reserved.
doi:10.1016/j.jcrysgro.2007.05.051

2. Experimental methods

We carried out crystallization of CsCl from agarose gel with in a way similar to what we reported previously [19–21]. First the solution of agarose was prepared by dissolving agarose (Fluka) in ultrapure water (Milli-Q Acdemic A10, electric resistivity 17.8 MΩ cm) with concentration 0.25 wt% in a waterbath of about 90 °C. CsCl of analytical purity (⩾99.5%) was dissolved in the hot agarose solution afterward with concentration varying from 0.6 to 60.0 wt%. The hot solution was filled into the space between two cleaned glass plates (normally a microscope slide and a cover glass). Gelation took place when the solution was cooled down. The separation between the glass plates was kept to 100 μm by four spacers. The cell was then placed in a glass chamber with relative humidity of about 80%. Supersaturation, the driving force for crystallization, was generated by evaporating water in the agarose gel through the edges of the glass plates. In our experiment, the water evaporation was not accurately controlled. Nevertheless, it was a slow process, especially when a salt crust of CsCl and agarose was formed along the edge of the glass plates. The salt crust acted as a sealing to prevent rapid evaporation of water from gel. Since the typical duration for *in situ* optical observation was usually 10–30 min, which was much shorter compared with the whole evaporation process (typically 15–30 h), the driving force for crystallization can be regarded as a constant in the duration of our optical observation. The aggregation process was observed *in situ* with a research optical microscope (Leitz Orthoplan-pol) equipped with CCD camera. The aggregate was further analyzed with a field-emission scanning electron microscope (FESEM) (LEO 1530VP) equipped with electron backscatter diffraction (EBSD) (EDAX). Meanwhile, the upper glass plate was removed already, and water in the gel had evaporated out. In EBSD experiment, when electron beam entered the surface layers of a crystalline solid, the electrons whose angle of incidence satisfying Bragg angle for some sets of lattice planes could undergo elastic scattering, and result in a strong, reinforced beam, known as Kikuchi line. The set of Kikuchi lines formed Kikuchi pattern, which embodied all angular relationships in a crystal and contained crystal symmetry. With the assistance of a computer software, crystal structure, orientation, and chemical identity of the single crystalline sample could be obtained.

3. Results and analysis

The aggregate of CsCl crystallites looks random and fractal like on large scale, as shown in Fig. 1(a). However, microscopically each branch possesses a deterministic zigzag feature. Fig. 1(b) shows the enlarged micrograph of the aggregate branch, where the zigzag feature can be easily seen. Occasionally nearly closed loops can be identified on the branch, as indicated by the arrows, which is usually not expected in diffusion-limited growth.

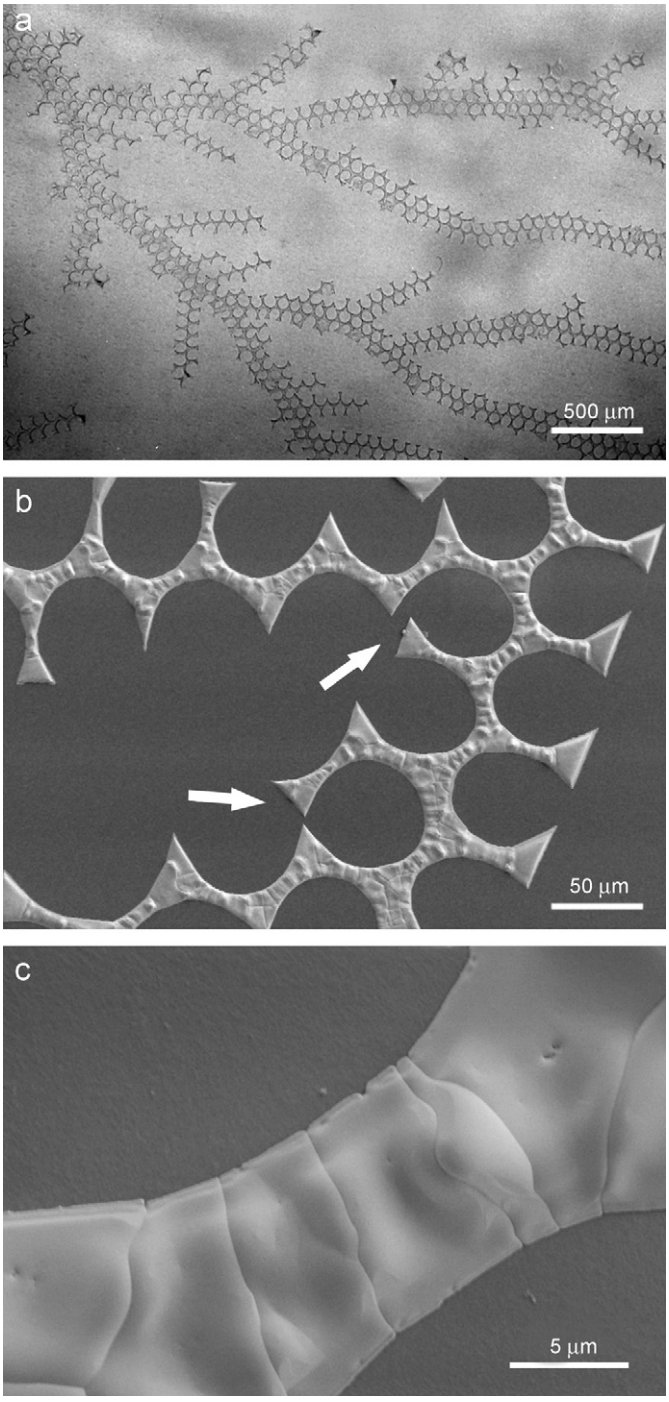

Fig. 1. (a) Optical micrograph of crystallite aggregate branches of cesium chloride. The CsCl concentration in the agarose gel is 1.0%. The bar represents 500 μm. (b) The SEM micrograph to show the zigzag branches. Some nearly closed loops can be found on the branch, as indicated by the arrows. Bumps can be identified on the branch as well. (c) SEM micrograph of the branch with higher magnification. Cracks appear on the top of the bumps.

The growing process of the zigzag branch recorded by *in situ* optical microscopy is shown in Fig. 2. As illustrated in Figs. 2(a) and (b), one corner of the pyramidal crystallite

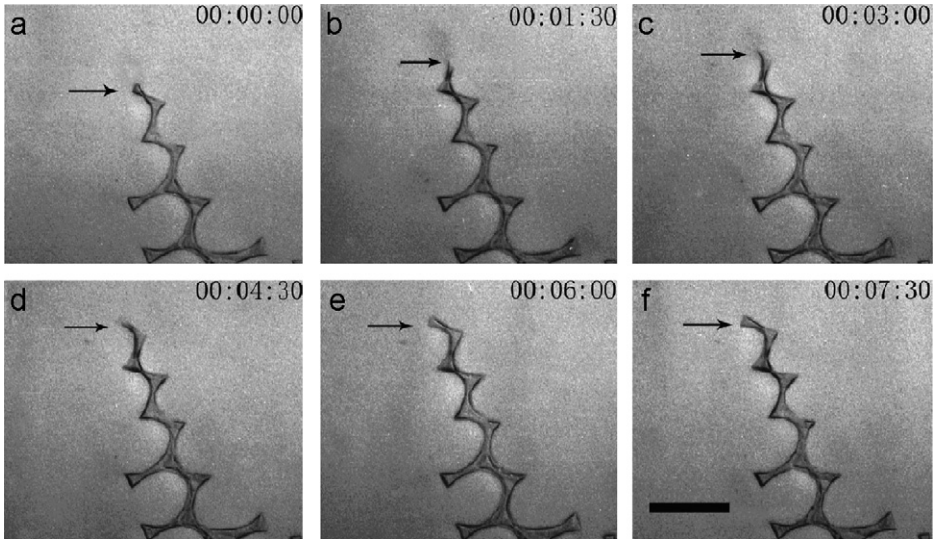

Fig. 2. Optical micrographs to illustrate the growing process of the zigzag branch. The digits on each frame stand for hour, minute, and second, respectively. The bar represents 50 μm.

grows faster and becomes cusp. As the cusp grows further, gradually it broadens and develops into a new pyramidal crystallite, which looks as if a mirror image of the previous one. Thereafter, as indicated in Figs. 2(c) and (d), one corner of the newly formed pyramidal crystallite grows faster and sharpens. Eventually a new cusp is once again generated, and evolves into a new crystallite. By repeating the above process a zigzag branch is generated.

To find out the formation mechanism of the zigzag branches, EBSD has been applied to determine the evolution of crystallographic orientation of the branch. Because the sample is insulating, the accumulation of electric charge on sample surface is evident, and drift may appear in SEM imaging. To decrease the overall measuring time and minimize the influence of drift, a narrow strip is selected on the zigzag branch, and EBSD is carried out only in this selected region. The result is shown in Fig. 3, where the color is scaled for different crystallographic orientations. One may find that from one pyramidal crystallite to the neighboring mirror-imaged one, the crystallographic orientation evolves continuously from [1 1 1] to [1 1 0] and then to [1 1 $\bar{1}$]. This scenario is exactly the same as what we observe in crystallization of NH_4Cl [19–20], where crystallites also form a regular zigzag branch, and the micro-X-ray-diffraction (XRD) from synchrotron radiation confirms the successive rotation of crystallo-graphic orientation.

Based on these experimental observations, we may understand the evolution of crystallographic orientation in formation of zigzag branches as follows. Suppose the crystallite initially contacts the substrate with ($\bar{1}$ $\bar{1}$ $\bar{1}$) and rotates with [1 $\bar{1}$ 0] as axis. In the meantime (1 1 1) is the top facet and (1 0 0) and (0 1 0) are the two side facets along the growth direction, as shown in Fig. 4(a). As crystallographic orientation rotates with axis [1 $\bar{1}$ 0], (1 1 1) inclines and (1 1 $\bar{1}$) gradually becomes larger (Fig. 4(b)). Further

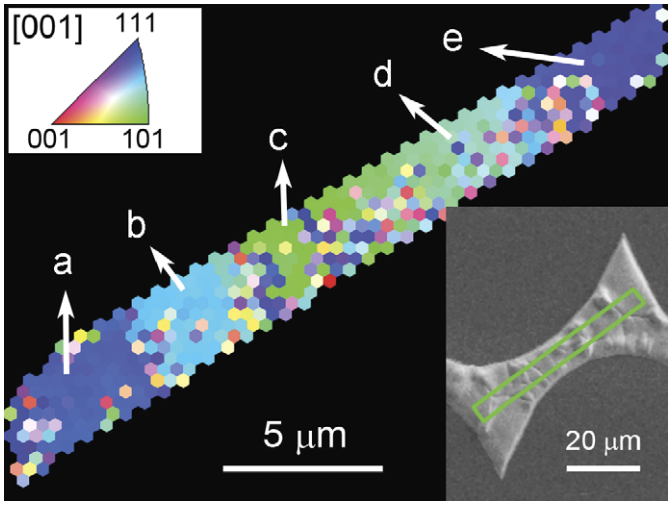

Fig. 3. The electron backscatter diffraction (EBSD) of the scrip region shown in the insert micrograph. The color is scaled to the crystallographic orientation. The crystallographic orientation at sites a–e correspond to that schematically illustrated in Fig. 4. One may easily find that the crystallographic orientation rotates continuously along the zigzag branch.

rotation leads to a special scenario where (1 1 1) and (1 1 $\bar{1}$) become symmetric, and edge [0 0 1] becomes in parallel to the substrate surface, as shown in Fig. 4(c). This scenario happens in the middle part of the long strip shown in Fig. 3 (marked as *c*), where the tips of two pyramids meet. Further rotation with [1 $\bar{1}$ 0] as axis makes the orientation reach a state as that shown in Fig. 4(d), and eventually to the scenario of Fig. 4(e). Meanwhile (1 1 $\bar{1}$) becomes the top facet, and whole crystallographic orientation becomes in mirror symmetry with that of Fig. 4(a). The crystallographic orientations in Figs. 4(a)–(e) correspond to that at sites *a–e* in Fig. 3, respectively.

Similar to what happened in crystallization of NH_4Cl [19–21], faceted (0 0 1) can also be easily observed in

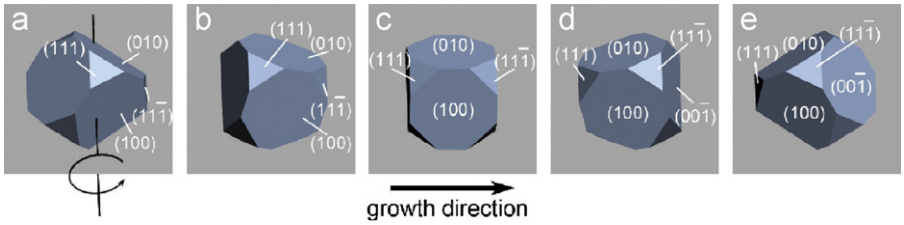

Fig. 4. The schematic diagrams to illustrate the evolution of the crystallographic orientation during the development of the branch. The rotation axis marked in (a) is (1 $\bar{1}$ 0).

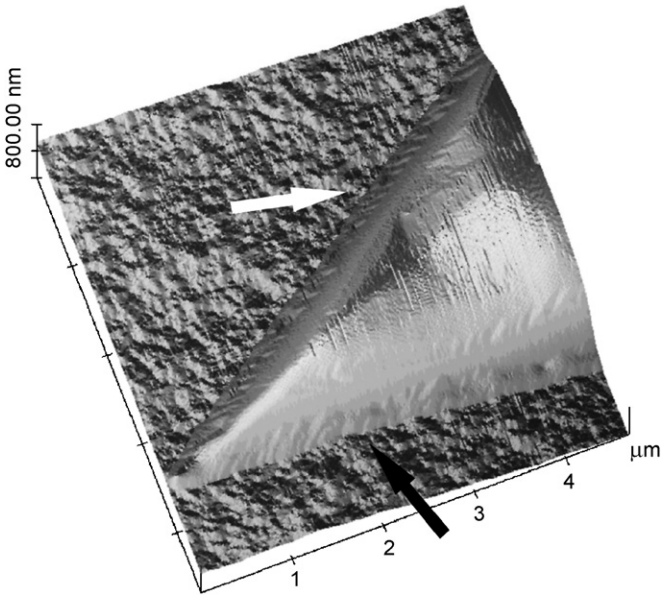

Fig. 5. AFM micrograph of the front tip of a zigzag branch. As indicated by the arrows, nucleation appears on the concave edge of the crystal facet and the substrate to initiate a crystaline step. The step moves uphill on (1 0 0) facets. Each crystalline layer is tilted because of the asymmetric interfacial tensions on the concave edge. Layer-by-layer the crystallographic orientation is continuously rotated.

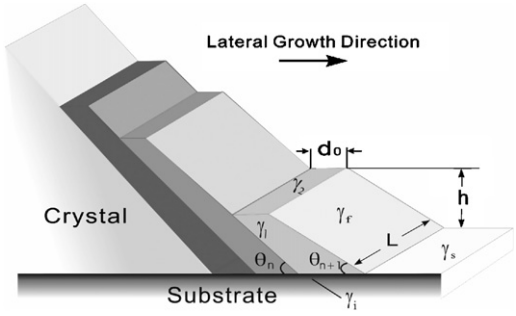

Fig. 6. The schematic diagram to illustrate the nucleation process on the concave edge. Once an embryo of nucleus appears on the concave edge (concave corner), the asymmetric surface tension underneath the embryo may twist its orientation, so each layer θ_n is slightly changed.

crystallization of CsCl. Our atomic force microscopy (AFM) observations indicate that nucleation on the concave edge of (0 0 1) facet and the glass substrate plays the role of step source to promote the growth of (0 0 1), as shown in Fig. 5. In other words, extension of cusp is sustained by successive generation of crystalline steps from the concave edge of crystal facet (0 0 1) and the substrate, followed by upward extension of steps on (0 0 1) facet. Fig. 5 provides an important clue to understand spontaneous, continuous rotation of crystallographic orientation.

4. Discussions

As we reported earlier, once nucleation takes place on the concave edge, the asymmetric surface tension underneath the embryo of nucleus may distort the crystallographic orientation of nucleus and hence the newborn crystalline layer. Once crystallization is sustained by successive nucleation on the concave edge, which is possible when driving force for crystallization is not very high, layer-by-layer, orientation of the crystallite is continuously rotated. To elucidate this more clearly, we may establish a model based on thermodynamics. Let γ_f, γ_s and γ_i stand for the energies of three interfaces: crystal–fluid, substrate–fluid and substrate–crystal, respectively. Fig. 6 schematically shows nucleation on the contact edge of (0 0 1) facet and glass substrate, as that illustrated in Fig. 5. Let θ_n represent the angle of the nth crystalline layer and the substrate. The height and thickness of the nascent nucleus (embryo) are defined as h and d_0, respectively. Because of the asymmetric surface tensions underneath the embryo, orientation of the embryo will be twisted by a small angle $\Delta\theta = \theta_{n+1} - \theta_n$. The total free energy for the formation of distorted nucleus on the concave edge can be expressed as [23]

$$\begin{aligned}\Delta G = & -\frac{hld_0}{v_c}\Delta\mu + \frac{1}{2}k_\mu\left(\frac{h}{d_0}\ \theta_n\Delta\theta\right)^2(hld_0) \\ & + 2hd_0\gamma_1 + ld_0(\gamma_2 + \gamma_i - \gamma_s) + lh(\theta_{n+1} \\ & - \theta_n)\gamma_f + \frac{1}{2}lh(\cot\theta_{n+1} - \cot\theta_n) \\ & \times(\gamma_i - \gamma_s - \gamma_2),\end{aligned}$$

where the first term denotes the change of chemical potential in crystallization, and the second term represents the bulk elastic energy due to the rotation of crystallographic orientation. The other terms are contributed by surface/interface energies. $\Delta\mu$ is the difference of chemical potential between the crystal phase and the fluid phase; k_μ is the elastic constant of the crystal and v_c is the atomic

volume. γ_1 and γ_2 represent, respectively, the surface energies of the side and top faces of the nucleus, as shown in Fig. 6. By minimizing the total free energy ΔG for a fixed volume, we may obtain the rotation of crystallographic orientation as

$$\Delta\theta = \frac{d_0}{k_\mu h^2}\left[(\gamma_f \cos\theta_n + \gamma_i - \gamma_s - \gamma_h/2) - \frac{\Delta\mu}{\gamma_h v_c}\frac{d\gamma_i}{d\theta} d_0 \sin^2\theta_n\right],$$

where $\gamma_h = \gamma_2 + \gamma_i - \gamma_s$ and is positive. Detail analysis indicates that $\Delta\theta$ is usually negative and does not change the sign in crystallization [23]. This means that once crystallization is promoted by successive nucleation at the concave corner as that shown in Fig. 6, crystalline facet will incline layer-by-layer until an equilibrium corner, θ_{eq}, is reached. θ_{eq} can be determined by $\Delta\theta = 0$, i.e.,

$$\gamma_f \cos\theta_{eq} + \gamma_i - \gamma_s = \frac{\gamma_h}{2} + \frac{\Delta\mu}{v_c}\frac{d \ln\gamma_h}{d\theta} d_0 \sin^2\theta_{eq}.$$

It should be pointed out that successive incline of crystallographic orientation indeed induces strain and increases the elastic energy. Yet this disadvantage can be compensated by reducing the interfacial area between the crystallite and the substrate. So eventually total free energy is decreased. For this reason the rotation process may spontaneously occur.

We still need to combine the formation of zigzag branch with successive rotation of crystallographic orientation discussed above. As indicated in Fig. 5, extension of the tip of pyramidal crystallite takes place via successive nucleation on the concave edges of two faceted {1 0 0} side faces and the substrate. The gradual inclining of crystalline layers on (0 0 1) and (0 1 0) facets is equivalent to the successive rotation of crystallographic orientation shown in Figs. 4(a)–(c). In fact, in Fig. 4(a) the angle between (0 1 0) facet (and (1 0 0)) and the substrate is 64°. By rotating the orientation with axis [1 $\bar{1}$ 0] to the scenario shown in Fig. 4(c), the angle between (0 1 0) and the substrate is decreased to 45°. It is noteworthy that for the scenario of Fig. 4(c), a new facet, (0 0 $\bar{1}$) appears on the growing front. Therefore in later development, successive nucleation along the concave edge of (0 0 $\bar{1}$) and the substrate will contribute to the continuous rotation of crystallographic orientation, until Fig. 4(e) is reached. It is known that for CsCl (for NH_4Cl as well), ⟨1 1 1⟩ is the preferred growth direction. Therefore, when crystal growth reaches scenario Fig. 4(e), successive growth will take place along either [1 $\bar{1}$ $\bar{1}$] or [$\bar{1}$ 1 $\bar{1}$], depending on the local concentration field. By repeating previous process, a zigzag branch with continuous rotation of crystallographic orientation is formed.

Now that the crystallographic orientation rotates continuously, one would expect that strain will be accumulated inside of the crystallite. For the growth of a strained crystal, it has been reported that bumps could be generated on an originally flat surface in order to release the accumulated stress [24,25]. In our experiments, bumps are indeed observed on the surface of the zigzag branches, as shown in Figs. 1(b) and (c). Moreover, crack-like grooves appear on the top of the bumps (Fig. 1(c)). These structures suggest that strain/stress should be involved in crystallization.

It is known that the growth of crystalline thin film may start by forming islands (nucleation) first, followed by horizontal extension of islands on the substrate [26–29]. The islands can be compact disks or droplets, and they can also be ramified and fractal-like clusters [28–31]. In previous studies of interfacial growth, despite the accomplishments in understanding thin film growth mechanism, however, little attention has been paid to how interfacial tensions affect the horizontal expansion of a crystalline island on a substrate of different material, especially for the scenario that the lateral expansion is motivated by repeated nucleation on the concave edge of crystalline facet and substrate. The experimental observations presented in this paper provide an example that once lateral growth is sustained by successive nucleation on the concave edge of crystallite facet and substrate, the crystallographic orientation can be continuously rotated, and a regular morphology with long-range order will be expected.

5. Conclusion

We report in this article the formation mechanism for the regularly zigzag branch of CsCl crystallites on a foreign substrate. Structural and morphological analyses indicate that the crystallographic orientation of the crystallite rotates continuously during lateral extension process, leading to a regular zigzag branch with long-range order on tens of micrometer scale. We suggest that this growth phenomenon reveals a possible universal lateral growth mode, and should be considered when the corner-mediated successive nucleation becomes important in lateral extension process of crystalline islands.

Acknowledgments

This work was supported by the grants from the Ministry of Science and Technology of China (G2004CB619005) and the National Science Foundation of China (Nos. 10021001 and 10625417).

References

[1] K. Brunner, Rep. Prog. Phys. 65 (2002) 27.
[2] M.T. Lung, C.H. Lam, L.M. Sander, Phys. Rev. Lett. 95 (2005) 086102.
[3] A. Ohtake, N. Koguchi, Appl. Phys. Lett. 89 (2006) 083108.
[4] C.R. Li, X.O. Zhang, Z.X. Cao, Science 309 (2005) 909.
[5] X.N. Zhang, C.R. Li, Z. Zhang, et al., Appl. Phys. Lett. 85 (2004) 3570.
[6] C.H. Chiu, Phys. Rev. B 69 (2004) 165413.
[7] K.G. Eyink, D.H. Tomich, J.J. Pitz, et al., Appl. Phys. Lett. 88 (2006) 163113.

[8] J.R.R. Bortoleto, H.R. Gutierrez, M.A. Cotta, et al., Appl. Phys. Lett. 87 (2005) 013105.
[9] R.F. Sabiryanov, M.T. Larsson, K.J. Cho, et al., Phys. Rev. B 67 (2003) 125412.
[10] O.G. Schmidt, N.Y. Jin-Phillipp, C. Lange, et al., Appl. Phys. Lett. 77 (2000) 4139.
[11] V.C. Elarde, T.S. Yeoh, R. Rangarajan, et al., J. Crystal Growth 272 (2004) 148.
[12] X.B. Zhang, R.D. Heller, J.H. Ryou, et al., J. Appl. Phys. 100 (2006) 043511.
[13] M. Dove, J.J. De Yoreo, S. Weiner (Eds.), Biomineralization, Reviews in Mineralogy and Geochemistry, vol. 54, Mineral Soc. Am., Washington, DC, 2003.
[14] H. Jiang, X.-Y. Liu, C.T. Lim, C.Y. Hsu, Appl. Phys. Lett. 86 (2005) 163901.
[15] R. Hiremath, J.A. Basile, S.W. Varney, et al., J. Am. Chem. Soc. 127 (2005) 18321.
[16] O.Y. Jianming, Prog. Chem. 17 (2005) 931.
[17] S. Kewalramani, G. Evmenenko, C.J. Yu, et al., Surf. Sci. 591 (2005) L286.
[18] D. Volkmer, M. Fricke, C. Agena, et al., J. Mater. Chem. 14 (2004) 2249.
[19] M. Wang, X.-Y. Liu, C. Strom, N.-B. Ming, P. Bennema, Phys. Rev. Lett. 80 (1998) 3089.
[20] D.-W. Li, M. Wang, P. Liu, R.-W. Peng, N.-B. Ming, J. Phys. Chem. B 107 (2003) 96.
[21] M. Wang, D.-W. Li, D.-J. Shu, P. Bennema, Y.-W. Mao, W. Pan, N.-B. Ming, Phys. Rev. Lett. 94 (2005) 125505.
[22] X.Y. Liu, Mu Wang, D.W. Li, C.S. Strom, P. Bennema, N.B. Ming, J. Crystal Growth 208 (2000) 687.
[23] D.-J. Shu, M. Wang, F. Liu, Z.Y. Zhang, R.-W. Peng, R. Zhang, N.B. Ming, J. Phys. Chem. C 111 (2007) 1071.
[24] J. Berrhar, et al., Phys. Rev. B 46 (1992) 13487.
[25] W.H. Yang, D.J. Srolovitz, Phys. Rev. Lett. 71 (1993) 1593.
[26] A. Pimpinelli, J. Villain, Physics of Crystal Growth, Cambridge University Press, Cambridge, 1998.
[27] I.V. Markov, Crystal Growth for Beginners: Fundamentals of Nucleation, Crystal Growth and Epitaxy, World Scientific, Singapore, 1995.
[28] H. Brune, C. Romainczyk, H. Roder, K. Kern, Nature 369 (1994) 469.
[29] F.-J.M. zu Heringdorf, M.C. Reuter, R.M. Tromp, Nature 412 (2001) 517.
[30] Z. Zhang, M.G. Lagally, Science 276 (1997) 377.
[31] N.-B. Ming, M. Wang, R.-W. Peng, Phys. Rev. E 48 (1993) 621.